Effects of ionenes on structure and catalytic activity of cobalt phthalocyanine. Part 6. Hydrogen peroxide accumulation

EFFECTS OF IONENES ON STRUCTURE AND CATALYTIC ACTIVITY OF COBALT PHTHALOCYANINE PART 6. HYDROGEN PEROXIDE ACCUMULATION*

JOKE VAN WELZEN, ALEX M. VAN HERK, HANS KRAMER and ANTON L. GERMAN**,

Laboratory of Polymer Chemistry, Eindhoven University of Technology, P.O. Box 513, 5600 MB Eindhoven (The Netherlands)

(Received May 18, 1989; revised August 8, 1989)

Summary

Accumulation of hydrogen peroxide during the catalytic oxidation of 2-mercaptoethanol in the presence of $CoPc(NaSO_3)_4$/2,4-ionene was investigated. It appeared to be the result of H_2O_2 formation via the catalytic reaction step and subsequent decomposition by further reaction with thiol.

The decomposition process was found to follow first-order kinetics in both H_2O_2 and RS^-, whereas the formation step could be described by a two-substrate Michaelis–Menten rate equation. Simulated accumulation profiles were in good agreement with experimental data and appeared to depend largely on Co catalyst, oxygen and initial thiol concentrations.

It was shown that accumulation of H_2O_2 causes a deviation of reaction stoichiometry from RSH: $O_2 = 4:1$. Experimentally determined oxygen uptake rate curves could be satisfactorily predicted when H_2O_2 accumulation effects were included in the calculation model.

Introduction

In our laboratory, extensive research is being carried out on the effects exerted by polymers, in particular ionenes (**1**), on the cobalt phthalocyanine (**2**) catalyzed thiol autoxidation [1–5]. Both by structural [1–3] and kinetic [4, 5] investigations we have attempted to elucidate the mechanism of this polymer-catalyzed process.

Our first detailed kinetic study [4] revealed that the process can be described neatly by the two-substrate Michaelis–Menten rate law, where the two substrates are thiol (2-mercaptoethanol) and oxygen.

In order to obtain better insight into the process mechanism, it is necessary to study the effects of various reaction conditions, such as pH, type of polymer and type of thiol, on the kinetic parameters. However, to carry out

*Part 5: see [1].

**Author to whom correspondence should be addressed.

0304-5102/90/$3.50

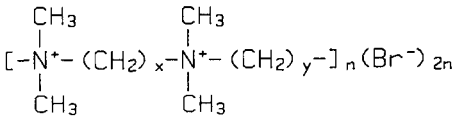

1: *x,y*-ionene

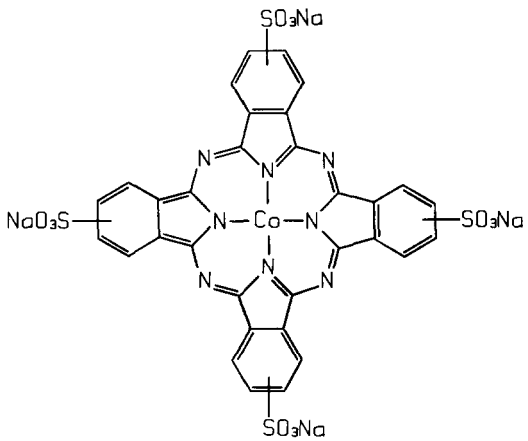

2: cobalt phthalocyanine–tetrasodiumsulfonate, $CoPc(NaSO_3)_4$

these investigations successfully, we first need a complete understanding of side-reactions, since these can obviously disturb the reaction kinetics.

It has been established previously [4, 6] that, during the ionene-catalyzed thiol oxidation, predominantly one side-reaction occurs, *viz.* formation of hydrogen peroxide (Scheme 1).

$$2RSH + O_2 \xrightarrow{v_f} RSSR + H_2O_2 \quad (1a)$$

$$2RSH + H_2O_2 \xrightarrow{v_d} RSSR + 2H_2O \quad (1b)$$

$$4RSH + O_2 \longrightarrow 2RSSR + 2H_2O \quad (1c)$$

Scheme 1.

Accumulation of this product indeed was found to cause deviations of the experimental rate profiles from the curves predicted by the Michaelis–Menten model [4], especially at low substrate concentrations. Therefore, we here present a separate study of the hydrogen peroxide related reactions.

Experimental

Ionene synthesis

2,4-Ionene (**1**) was synthesized according to the method of Brouwer *et al.* [6]; the M_n value was 8600, determined by the titration method described in [7].

Other materials

$CoPc(NaSO_3)_4$ (**2**) was kindly provided by Dr. T. P. M. Beelen and was prepared according to an adaptation by Zwart *et al.* [8] of the method of Weber and Busch [9].

2-Mercaptoethanol (Fluka) was distilled prior to use, all other chemicals were of analytical purity and used without further purification.

Kinetic measurements of the reaction of H_2O_2 + RSH

The kinetics of reaction (1b) (or Scheme 2) were determined by investigating the absorbance increase at 280 nm with time (due to disulfide formation) as a function of thiol and hydrogen peroxide concentrations. The obtained absorbance *versus* time curves were analyzed by means of the computer program FORK (First Order Reaction Kinetics), a modified version of the non-linear least squares program LSG of Detar [10].

When an (at least 10-fold) excess of thiol was used, the order in hydrogen peroxide could be determined. Its value appeared to be equal to 1, the data fitting very well the equation

$$-d[H_2O_2]/dt = k'[H_2O_2] \quad (1)$$

Using various excess concentrations of RS^-, a set of k' values was obtained, yielding the actual rate constant k according to:

$$k' = k[RS^-] \quad (2)$$

Analogously, k was determined by using various excess concentrations of H_2O_2.

Absorbance measurements were performed with a Hewlett Packard 8451A diode array spectrophotometer. A 1.000 cm quartz cuvette was used, thermostatted at 25.0 ± 0.1 °C. Reactions were carried out under nitrogen atmosphere at pH 8, 8.3, 8.85 and 9, using TRIS-buffers (tris(hydroxymethyl)aminomethane) with an ionic strength of 0.1 mol dm^{-3}.

H_2O_2 accumulation measurements

During several catalytic oxidation experiments, H_2O_2 accumulation was determined as a function of time. Samples of 0.5 ml were taken from the reaction vessel by means of a syringe containing 0.5 ml HCl (3 mol dm^{-3}) in order to quench further reactions (see Discussion). The H_2O_2 content of the samples was measured spectrophotometrically using $TiCl_3$–H_2O_2 as reagent [11].

Catalytic activity measurements

Catalytic oxidation experiments were performed as described previously [4].

Simulation procedure

H_2O_2 accumulation curves and oxygen uptake rate profiles were calculated numerically on the basis of eqns. (3) to (5), derived from

Scheme 1:

$$d[H_2O_2]/dt = v_f - v_d \quad (3)$$

$$d[RSH]/dt = -2(v_f + v_d) \quad (4)$$

$$d[O_2]/dt = -v_f \quad (5)$$

where v_f and v_d are calculated according to eqns. (6) and (7) (see Results and discussion). Numeric integration was carried out over time steps of typically 2 s (≤2.5% of total reaction time).

Results and discussion

Hydrogen peroxide decomposition

From Scheme 1, it is clear that accumulation of hydrogen peroxide can occur when its formation via step (1a) proceeds at a higher rate than its decomposition via (1b). Therefore, kinetic data of both processes are desired as a function of reaction conditions, in order to be able to predict the peroxide accumulation under all conditions and the accompanying deviation of the overall reaction stoichiometry.

We will first discuss the second reaction step, (1b), which has been described [12 – 15] to follow an S_N2-type mechanism according to Scheme 2.

$$RS^- + H_2O_2 \longrightarrow RSOH + OH^-$$

$$RS^- + RSOH \longrightarrow RSSR + OH^-$$

$$2RS^- + H_2O_2 \xrightarrow{v_d} RSSR + 2OH^-$$

Scheme 2.

Barton *et al.* [12] investigated the kinetics of the conversion of cysteine and cysteamine according to this process. They found a rate dependence that was first order in both H_2O_2 and thiolate anion. The reaction rate constants, calculated according to:

$$v_d = -d[H_2O_2]/dt = k[RS^-][H_2O_2] \quad (6)$$

were reported to be 10 and 12.4 $dm^3\,mol^{-1}\,s^{-1}$ for cysteamine and cysteine, respectively.

The same kinetic relationship was also mentioned for the conversion of *n*-propylthiol in a study of Giles *et al.* [14, 15]. They reported a rate constant of 7 $dm^3\,mol^{-1}\,s^{-1}$ (at 25 °C).

Since 2-mercaptoethanol is the substrate used in our kinetic investigations, we examined the kinetics of the reaction of Scheme 2 for this thiol. The rate of the process was determined spectrophotometrically as a function of thiol and H_2O_2 concentration, while the effects of $CoPc(NaSO_3)_4$ and 2,4-ionene were also studied.

The following results were obtained:

— at pH-values above 9, the reaction rate was too high to study the kinetics of the process by our method;

— for $pH \leq 9$, the reaction appeared to be first order in H_2O_2 and thiolate anion;

— the rate constant according to eqn. (6) was found to be 4.3 ± 0.8 dm^3 mol^{-1} s^{-1} when an excess of thiol was used, and 12 ± 3 dm^3 mol^{-1} s^{-1} with an excess of hydrogen peroxide; the result obtained with excess of peroxide is though to be less reliable, since under these conditions a secondary reaction, probably photo-oxidation of the thiol [16], was observed, seriously disturbing the kinetic measurements; in Fig. 1 the effect of the secondary process is illustrated;

— addition of Co-phthalocyanine and/or ionene had no detectable effect on reaction rate.

The latter finding in particular is very important: since the rate of formation of the peroxide (step (1a), Scheme 1) depends on both the cobalt and the ionene concentrations, whereas its decomposition rate (Scheme 2 or step (1b) in Scheme 1) apparently does not, the amount of accumulated hydrogen peroxide will thus depend on these quantities. Moreover, accumulation will of course depend on the initial concentrations of thiol and oxygen.

Simulation of hydrogen peroxide accumulation

In the preceding section it was shown that the kinetics of step (1b) of Scheme 1 can be described by eqn (6) with $k \approx 4$ dm^3 mol^{-1} s^{-1}. For step (1a) it has been demonstrated [4, 5] that the kinetics follow the two-substrate

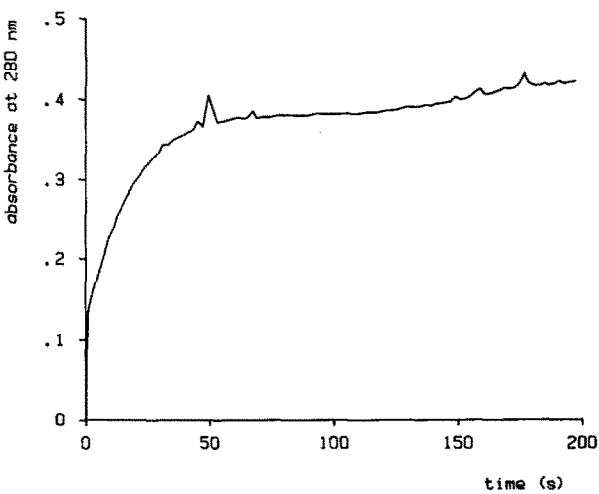

Fig. 1. Variation in absorbance at 280 nm with time, during the reaction of an excess of H_2O_2 with 2-mercaptoethanol. Conditions: nitrogen atmosphere, $[H_2O_2]_0 = 0.11$ mol dm^{-3}, $[RSH]_0 = 4.7 \times 10^{-3}$ mol dm^{-3}, pH = 8.0.

Michaelis–Menten model, resulting in the rate equation:

$$v_f = d[H_2O_2]/dt = \frac{C_1[Co]}{1 + C_2/[O_2] + C_3/[RS^-] + C_2C_4/([RS^-][O_2])} \quad (7)$$

where C_1–C_4 are complex rate constants. (In order to facilitate comparison with [4, 5], it must be noted that C_1 here equals k_3, the rate constant for product formation from the ternary O_2–Co–RS^- complex, since v_f is expressed in moles of peroxide per liter per second instead of moles of thiol per liter per second as was done in [4, 5].)

Thus, for a given initial concentration of thiol, given concentrations of oxygen and $CoPc(NaSO_3)_4$ and with values for C_1–C_4 at the applied pH, the accumulation of hydrogen peroxide can be calculated by combining both kinetic relationships. Using the values for C_1–C_4 previously determined [5] at pH 8.85 and following the numerical calculation procedure described in the experimental section, the following results were obtained.

(1) Increasing the cobalt concentration leads to an increase in peroxide accumulation, as depicted in Fig. 2. This is the consequence of the fact that H_2O_2 formation (step (1a)) is accelerated by the catalyst, whereas the decomposition rate (step (1b)) is not affected.

(2) Analogously, increasing the oxygen concentration also causes enhancement of peroxide accumulation.

(3) Variation of the initial thiol concentration results in two types of H_2O_2 accumulation curves, as can be seen in Fig. 3A and B. At low $[RSH]_0$ (<0.04 mol dm^{-3}), the curve shows characteristics of pseudo-first order

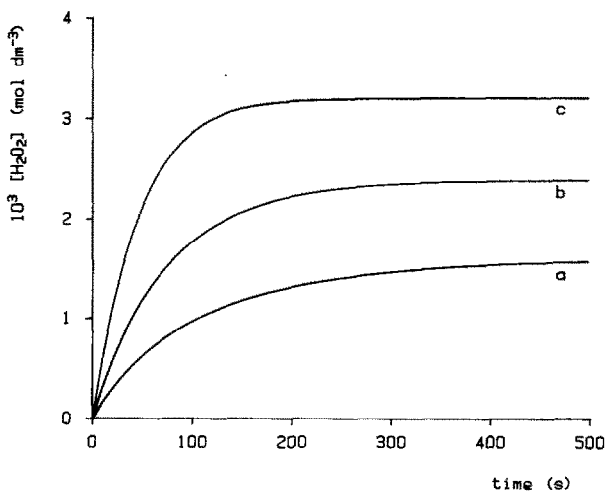

Fig. 2. Effect of varying the $CoPc(NaSO_3)_4$ concentration on the simulated H_2O_2 accumulation curves. Simulations based on eqns. (6) and (7), with $k = 4\ dm^3\ mol^{-1}\ s^{-1}$, $C_1 = 10^3\ s^{-1}$, $C_2 = 3 \times 10^{-4}\ dm^3\ mol^{-1}$, $C_3 = 9 \times 10^{-3}\ dm^3\ mol^{-1}$ and $C_4 = 5 \times 10^{-2}\ dm^3\ mol^{-1}$. Conditions: $[O_2] = 0.00055$ mol dm^{-3}, $[RSH]_0 = 0.01$ mol dm^{-3}, pH = 8.85; $[Co] = 10^{-7}$ (a), 2×10^{-7} (b) and 4×10^{-7} mol dm^{-3} (c).

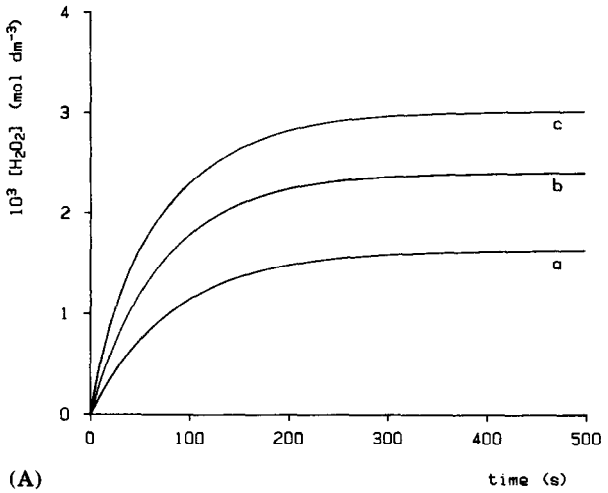

(A)

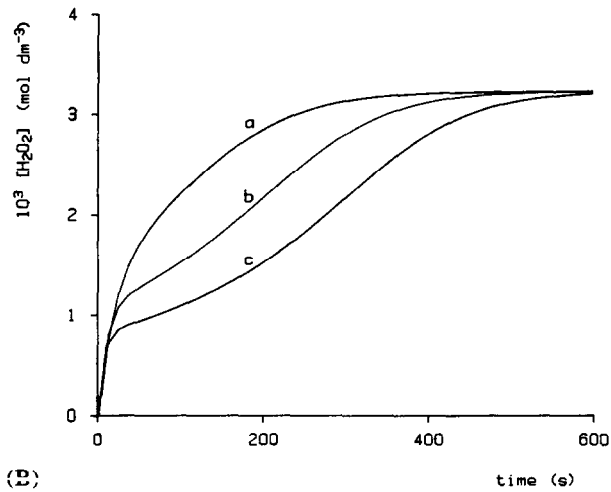

(B)

Fig. 3. Effect of varying the initial thiol concentration on the simulated H_2O_2 accumulation curves. Kinetic parameters as in Fig. 2. Conditions: $[O_2] = 0.00055$ mol dm^{-3}, $[Co] = 2 \times 10^{-7}$ mol dm^{-3}, pH = 8.85. (A) Low $[RSH]_0$: 0.005 (a), 0.01 (b) and 0.02 mol dm^{-3} (c). (B) High $[RSH]_0$: 0.04 (a), 0.08 (b) and 0.12 mol dm^{-3} (c).

kinetics; increasing the thiol concentration in this region leads to an increase in peroxide accumulation. However, at high $[RSH]_0$ the shape of the curve changes: first, the hydrogen peroxide concentration rapidly increases (with an initial rate that is independent of thiol concentration); then, when a certain level is reached (which decreases as $[RSH]_0$ increases), the amount of accumulated H_2O_2 remains almost constant for a period; finally, the hydrogen peroxide concentration starts to increase again but at a relatively low rate.

These complicated accumulation profiles are due to the fact that the kinetics of the formation of H_2O_2 (step (1a), eqn. (7)) change from zero to first order in thiolate anion as thiol concentration decreases. The H_2O_2 'plateau' at high thiol concentration and low conversion indicates that a steady state is reached, *i.e.* v_f equals v_d in this region.

Accumulation measurements

To verify if the kinetic theory described above is correct, H_2O_2 accumulation curves were measured as a function of thiol, oxygen and cobalt

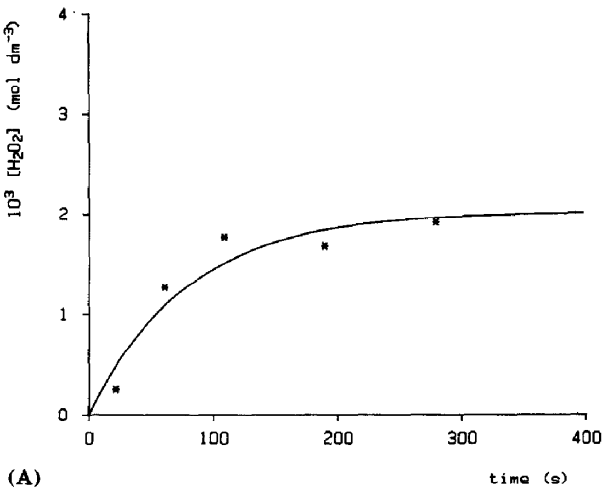

(A)

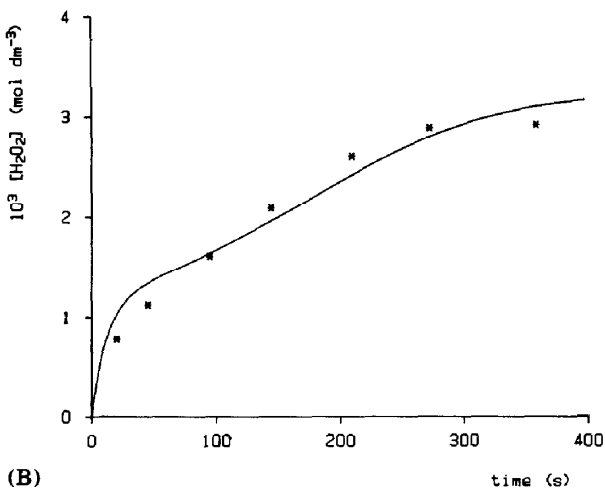

(B)

Fig. 4. Comparison of experimentally determined (*) and simulated (—) H_2O_2 accumulation curves. Kinetic parameters as in Fig. 2. Conditions: $[O_2] = 0.00055$ mol dm^{-3}, $[Co] = 2 \times 10^{-7}$ mol dm^{-3}, pH = 8.85; $[RSH]_0 = 0.0071$ (A) and 0.071 mol dm^{-3} (B).

concentrations, by analyzing samples of the reaction mixtures during the catalytic conversion of thiol.

It was found that, especially for low initial thiol concentrations, these experimental curves were in very good agreement with the simulated profiles; typical examples are shown in Fig. 4A and B.

For high $[RSH]_0$ at low conversions, the measured amounts of peroxide were often too low compared with the calculated values. This was found to be a result of inadequate mixing of the samples with the concentrated acid that was added in order to quench further reaction (see Experimental section). At the moment the sample is taken out of the reactor, the oxygen concentration immediately decreases to zero, stopping the H_2O_2 formation process. However, as long as the sample is not sufficiently mixed with the hydrochloric acid, the decomposition reaction of peroxide still continues, at a relatively high rate due to the high thiol concentration. Therefore, the amount of H_2O_2 that is measured will be too low. Nevertheless, the shape of the obtained experimental curves is very similar to the shape of the calculated ones. It can thus be concluded that the kinetic model satisfactorily describes the H_2O_2 side reactions.

Influence of H_2O_2 accumulation on catalytic measurements

In our laboratory, the kinetics of catalytic thiol conversion are studied by measuring oxygen uptake rates. Since the overall stoichiometry of reaction (1c) will no longer be valid when peroxide is accumulated, the effects of accumulation on oxygen flow curves had to be studied. Figure 5 shows three of these curves, one experimentally determined (a), the other two simulated, (b) without and (c) with a correction for H_2O_2 accumulation.

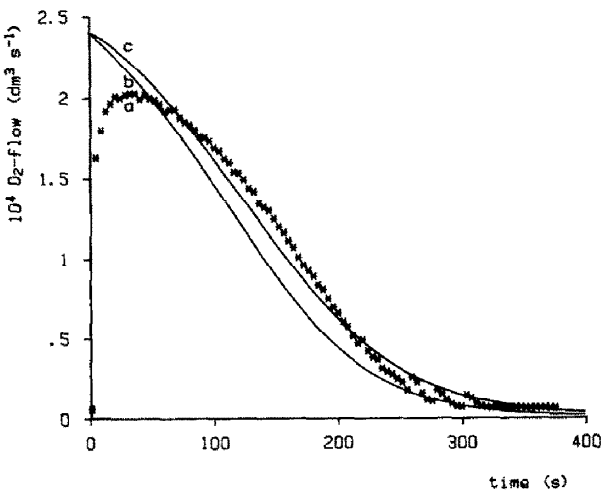

Fig. 5. Oxygen uptake rate curves as experimentally determined (a) and simulated (b, c). Simulation (b) is based on eqn. (7) and a constant stoichiometry of $RSH:O_2 = 4:1$, simulation (c) is based on eqns. (6) and (7). Kinetic parameters as in Fig. 2. Conditions: $[O_2] = 0.0011$ mol dm^{-3}, $[Co] = 2 \times 10^{-7}$ mol dm^{-3}, $[RSH]_0 = 0.051$ mol dm^{-3}, pH = 8.85.

At the start of the reaction both simulations deviate largely from the experimental curve. This is due to the experimental procedure: the reaction is started by adding the thiol to the closed reaction vessel, which leads to a gas pressure increase; therefore, detection of oxygen consumption can only start after a volume of oxygen is consumed that equals the injected volume of thiol. After this point has been reached, the experimental curve reveals a profile similar to the simulated curves.

Curve (5b) represents a calculation based on the assumption that no H_2O_2 is accumulated, so that the stoichiometry of $RSH:O_2 = 4:1$ is maintained during the entire process. It is evident that, at high conversions, the experimental curve (5a) shows a considerable deviation from this model curve, as was expected. This illustrates very well that, in general, kinetic studies are to be based on initial rates, in which the effect of by-products is not yet detectable.

However, in this process it is now possible to obtain more kinetic data from one flow curve, since the complete curve can be analyzed by means of the kinetic model including peroxide accumulation effects. Figure 5 shows that the calculated curve according to this model (5c) is in good agreement with the experimental result (5a).

Conclusions

In order to describe complete oxygen uptake rate curves for the catalytic oxidation of thiol, it is necessary to include the H_2O_2 accumulation process in the kinetic equations. Formation of the peroxide can be described by the Michaelis–Menten rate eqn. (7), whereas the H_2O_2 decomposition reaction follows kinetics that are first order in both H_2O_2 and thiolate anion.

Since, in contrast to the formation rate, the decomposition rate is independent of catalyst and oxygen concentrations, the degree of peroxide accumulation depends on these concentrations. Furthermore, accumulation largely depends on the initial thiol concentration. Accumulation curves can be very well predicted on the basis of the above-mentioned kinetic equations.

References

1 J. van Welzen, A. M. van Herk and A. L. German, *Makromol. Chem.*, accepted for publication.
2 J. van Welzen, A. M. van Herk and A. L. German, *Makromol. Chem., 189* (1988) 587.
3 V. van Welzen, A. M. van Herk and A. L. German, *Makromol. Chem., 188* (1987) 1923.
4 A. M. van Herk, A. H. J. Tullemans, J. van Welzen and A. L. German, *J. Mol. Catal., 44* (1988) 269.
5 A. M. van Herk, K. H. van Streun, J. van Welzen and A. L. German, *British Polym. J.*, accepted for publication.
6 W. M. Brouwer, P. Piet and A. L. German, *J. Mol. Catal., 31* (1985) 169.
7 K. H. van Streun, P. Piet and A. L. German, *Eur. Polym. J., 23* (1987) 941.

8 J. Zwart, H. C. van der Weide, N. Bröker, C. Rummens, G. C. A. Schuit and A. L. German, *J. Mol. Catal., 3* (1977–78) 151.
9 J. H. Weber and P. H. Busch, *Inorg. Chem., 4* (1965) 469.
10 D. F. Detar, *Computer Programs for Chemistry,* Vol. 1, Benjamin, New York, 1969.
11 A. C. Egerton, A. J. Everett, G. J. Minkoff, S. Rudrakanchana and K. C. Salooja, *Anal. Chim. Acta, 10* (1954) 422.
12 J. P. Barton, J. E. Packer and R. J. Sims, *J. Chem. Soc., Perkin Trans. 2,* (1973) 1547.
13 F. A. Davis, P. L. Billmers, *J. Am. Chem. Soc., 103* (1981) 7016.
14 D. W. Giles, J. A. Cha, P. K. Lim, *Chem. Eng. Sci., 41* (1986) 3129.
15 P. K. Lim, D. W. Giles, J. A. Cha, *Chem. Eng. Sci., 41* (1986) 3141.
16 S. Patai (ed.), *The Chemistry of the Thiol Group,* Wiley London, 1974; Part 1, Chapt. 10 and Part 2, Chapt. 17.